Journal of Environmental Chemical Engineering 12 (2024) 112474

Contents lists available at ScienceDirect

Journal of Environmental Chemical Engineering

journal homepage: www.elsevier.com/locate/jece

Plastic waste recycling in additive manufacturing: Recovery of polypropylene from WEEE for the production of 3D printing filaments

Andrea Spirio [a], Rossella Arrigo [b], Alberto Frache [b], Letizia Tuccinardi [a,*], Riccardo Tuffi [a]

[a] Department for Sustainability, ENEA Casaccia Research Center, Rome, Italy
[b] Department of Applied Science and Technology, Politecnico di Torino, Alessandria, Italy

ARTICLE INFO

Keywords:
Mechanical recycling
Polypropylene
WEEE plastics
3D printing
Fused Filament Fabrication

ABSTRACT

The inefficient management of wastes recovered from electric and electronic apparatuses (the so-called WEEE or e-waste) has become a severe global concern in the last years, since the indiscriminate accumulation of wastes containing hazardous material poses serious risks for the environmental, as well as for the human health. Despite the continuous development of innovative and efficient technologies for the mechanical recycling of WEEE plastics, the effective re-utilization of these fractions is often limited by their poor value-added. In this work, we propose a strategy for the valorization of a typical WEEE plastic stream recovered from small appliances (mainly composed on polypropylene filled with talc particles) through the formulation of filaments suitable for Fused Filament Fabrication (FFF) 3D printing processes. Preliminary spectroscopic analyses on the WEEE plastics allowed separating the sample in two streams, according to the different content of talc. Both streams were first characterized from a rheological point of view, aiming at assessing their 3D printability. Then, the mechanical properties and the morphology of the filaments (obtained after a close optimization of the extrusion conditions) were evaluated; the obtained results indicated the achievement of a regular geometry and mechanical properties comparable to those of commercial filaments. Finally, 3D printed specimens showed a satisfactory quality in terms of resolution and definition, demonstrating the possibility of profitably enhancing the value-added of WEEE plastics, using them as feedstock to produce sustainable 3D printing filaments.

1. Introduction

In recent years, the continuous introduction into the market of new electric and electronic equipment (EEE, most of them having a short lifetime) has led to the generation of a huge amount of waste from the discarded items [1–3]. According to the last available data, in Europe (considering the 27 Member States, Norway, United Kingdom, Switzerland and Iceland) the documented collection of the so-called WEEE (i.e., waste electric and electronic equipment) or e-waste, showed an increase of 1.8 Mt in the last decade, passing from 3.8 Mt (2010) to 5.6 Mt (2021), with a production of about 10.5 kg of wastes for inhabitant [4]. The depicted scenario is even more severe considering that the typical recycling rate of WEEE is very low (about 17 wt% of the total collected amount in 2019), due to the extremely high intrinsic complexity of both collection and recycling processes, making the reuse and/or recycle strategies challenging from both technological and economic point of view [5,6].

The first issue strongly affecting the efficient recycling of WEEE is related to the separation of the plastic fraction from the other materials [7,8]. In fact, the WEEE streams typically consists of variable quantity of plastic materials (mainly thermoplastics, about 10–50 wt%), depending on the type of appliance [9], mixed with metals and glass. Besides, since WEEE consists of many components and equipment of different size, shapes and applications, the recovered plastic streams are extremely heterogeneous, and further sorting steps are imperative for obtaining homogeneous materials, suitable for the successive recycling processes [10–12]. In this context, several technologies allowing an efficient separation and sorting of the plastic streams have been patented in the last decade [13]. On the other hand, it is important to note that plastics recovered from WEEE could contain hazardous substances which need to be removed with specific treatments [14,15]. Most commonly, these plastics are separated and sent to energy recovery or landfill [16]. Therefore, only 50–60 wt% of the input material to WEEE plastic recycling facilities is effectively recycled [16]. Added to these are the upstream losses due to low WEEE collection rate and losses at WEEE pre-processing stages. Only a small part of WEEE plastics resulting in

* Corresponding author.
E-mail address: letizia.tuccinardi@enea.it (L. Tuccinardi).

https://doi.org/10.1016/j.jece.2024.112474
Received 22 November 2023; Received in revised form 8 March 2024; Accepted 9 March 2024
Available online 19 March 2024

Europe is recycled with the consequence of a significant wastage of valuable materials. Furthermore, even if some manufacturing processes include the use of secondary raw materials from WEEE, they are usually considered low value plastics and their market is still not consolidated [13].

In conclusion, the full mechanical recycling of WEEE plastics is far from being exploited and this fraction is often left behind in favor of the more profitable recovery of metals and glass.

Hence, efficient management of WEEE is deemed as one of the most important global environmental challenges in the twenty-first century. Innovative technologies and strategies allowing an efficient recycling of the plastic fraction, as well as an effective re-utilization of the recovered materials through high value-added applications need to be implemented and developed. In recent years, additive manufacturing (or 3D printing) processes have emerged as innovative and eco-friendly manufacturing technologies. These processes can produce customized objects and parts having complex designs and geometries, allow to save energy and material compared to traditional processing methods [17,18]. Specifically, concerning the 3D printing technologies for thermoplastics, material extrusion-based methods (including fused filament fabrication, FFF) are the most used. Despite the limited selection in material recovery facilities (MRF) of polymeric materials that possess the appropriate characteristics of processability [19], quite recently, some studies are focusing on the exploitation of recycled thermoplastics for 3D printing applications [20–22]. These papers demonstrated the possibility of producing plastic objects using a more sustainable manufacturing approach, which involves the combination of materials recovered from waste and a low energy-consuming process. However, in the same way as printed components obtained from commercial filaments, also in the case of recycled plastics, it is imperative for the FFF process to select the suitable parameters to print specimens with optimum features in terms of porosity, strength, surface integrity and accuracy and consequently to ensure the above-mentioned sustainability of the process [23]. It has also been shown that plastics recovered from WEEE can be profitably valorized through the production of 3D printing filaments suitable for FFF processes [13,24,25]. As an example, [13] WEEE plastic from end-of-life printers (constituted predominantly by polycarbonate) used to produce 3D printed items, exhibited mechanical properties comparable to those of the same items based on commercially filaments. Furthermore, the LCA (life cycle assessment) studies suggested that the exploitation of WEEE plastics as feedstock for formulating 3D printing filaments instead of virgin polymers resulted in a reduction of about 30% in CO_2 emissions [13].

In this work, we propose a strategy of valorization of WEEE plastics from small appliances (mainly composed of polypropylene, PP) through the production of filaments for 3D printing process. PP can represent up to 57 wt% of the composition of the plastics used in EEE [16]. As known in literature, PP is not easily 3D printable, due to its unfavourable rheological and thermal characteristics [26]. However, the common presence of talc in PP used in EEE can provide a material with the proper processability and can help in overcoming the issues related to its typical high volumetric shrinkage associated with its semi-crystalline nature, as recently demonstrated with virgin PP [27]. Therefore, WEEE scraps were processed to obtain printable filaments and FFF printed parts. The optimization of the extrusion conditions allowed obtaining regular and stable filaments, having mechanical properties comparable to those of commercially available counterparts. PP-based recycled filament could be used in 3D printing process as a material with good physical properties (such as resistance to heat, chemicals, fatigue, and impact) for different items with the further advantage of using secondary raw materials, instead of virgin PP ones. The resolution and definition of the 3D specimens were qualitatively evaluated, confirming once again that the overall quality was very similar to that of specimens realized by using commercial filaments.

2. Materials and method

2.1. Materials

Approximately 4 kg of PP-WEEE plastic, belonging to the category of small appliances, was sampled from a WEEE MRF (Puli Ecol Recuperi Srl, Italy), as was already done in a previous work carried out by the authors [25]. The sample consisted of 5–10 cm plastic scraps, originating from different appliances.

In order to ensure a homogeneous plastic stream for the extrusion process, the sample underwent a product analysis by Fourier Transform Infrared - Attenuated Total Reflectance (FTIR-ATR) spectroscopy. All the scraps were analysed by 4300 Handheld FTIR (Agilent), acquiring the FTIR spectrum between 4000÷400 cm^{-1} at a resolution of 8 cm^{-1} and averaging 45 scans for each measurement. The FTIR spectra were compared with those of the instrument library. After the FTIR analysis, the sample was divided into three parts: PP characterized by a high concentration of inorganic additive (with an absorbance peak at 1014 cm^{-1}> 0.3, called PP-WEEE-HA), by low concentration of inorganic additive (with an absorbance peak at 1014 cm^{-1} < 0.3, called PP-WEEE-LA), foreign materials.

2.2. Preparation to analysis and processing

The scraps were coarsely cut with a hand lever shear (Peddinghaus 3BR6), aiming at obtaining a more homogeneous geometry and at reducing their dimension prior to the use of the cutting mill. Subsequently, the scraps were washed in a laboratory dishwasher (Mielabor 6773) at 70 °C with a common detergent to eliminate the grime on the plastics, such as dust, grease and glue, which were present in many scraps (Fig. 1a). Extremely dirty scraps were also manually cleaned with denatured ethanol. After rinsing with demineralized water, the materials were dried in an oven (WTB Binder E53) at 50 °C for 24 h.

The cutting mill used for grinding the samples was a Retsch SM 2000 with a 2.2 kW drive and 1500 min^{-1} rotor speed. The cleaned samples were divided into two portions: one was milled to a particle size lower than 4 mm for the extrusion process (Fig. 1b) and the other one (50 g) to a particle size lower than 0.5 mm for the physical-chemical characterization (Fig. 1c). Prior to this second grinding step, the 4 mm portion was manually mixed and quartering in a tray to guarantee a representative and homogeneous distribution of the sample for the analyses.

2.3. Preliminary characterization

2.3.1. Ultimate and proximate analysis

In the case of plastic/organic materials, ultimate analysis concerns the quantitative determination of Carbon (C), Hydrogen (H), Nitrogen (N), Sulphur (S), Oxygen (O). In this work, C, H, N and S were analyzed using a Macro VARIO Cube Elemental Analyser in accordance with a method described elsewhere [28], while O was calculated as the difference of all present elements and the ash content to 100 wt%.

WEEE plastics may contain flame retardants, mainly in the form of organobromine and organochlorine compounds [29]. Chlorine (Cl) and Bromine (Br) were determined according to the method and analysis reported in a previous work of the authors [25] through a calorimetric bomb (C5000 Berthelot-Mahler Calorimeter, IKA). The analysis of the resulting solution was carried out by ionic chromatography (883 Basic IC plus Metrohm Ion Cromatographer).

The total amount of inorganic species was reported as ash content determined by proximate analysis using a thermogravimetric and differential scanning calorimetry (TGA/DSC1, Mettler Toledo) instrument. Samples weighing approximately 40÷50 mg for each test were placed into an alumina crucible. Runs were carried out applying the thermal program reported in Table 1. Proximate analysis also provided information regarding the water content of the samples. Each measurement was performed with 3 replicas.

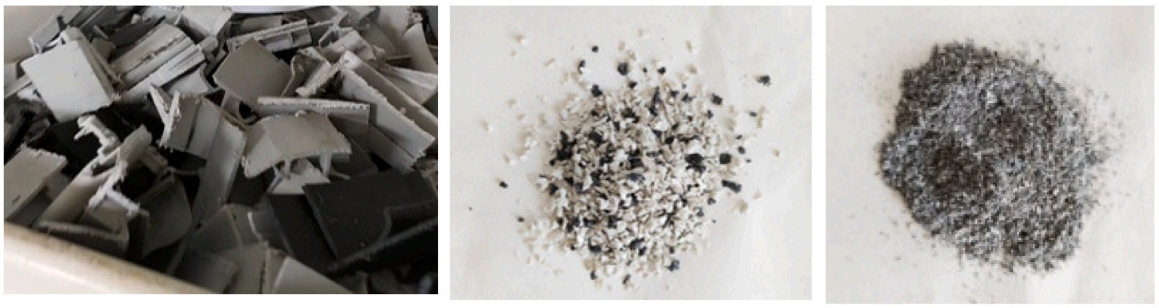

Fig. 1. Cleaned scraps (a); sample grinded < 4 mm (b); powder < 0.5 mm (c) of PP-WEEE-HA.

Table 1
TGA thermal program for proximate analysis.

	Temperature program			
Atmosphere	T_i (°C)	T_f (°C)	$\beta = dT/dt$ (°C·min^{-1})	Δt isotherm (min)
N_2 at 60 ml·min^{-1}	25		–	5
	25	105	20	–
	105		–	15
	105	900	20	–
	900		–	5
Air at 90 ml·min^{-1}	900		–	30

2.3.2. Thermal behavior

Thermal analysis was carried out with the Mettler-Toledo TGA/DSC1 with a standard temperature program (from 25 to 600 °C at 10 °C·min^{-1}) to define the melting temperature (T_m), the initial degradation temperature (determined from the first derivative of the DTG curve and corresponding to the beginning of the steep slope of TG curve, $T_{d,i}$) and the degradation peak temperature ($T_{d,p}$) of the samples. A quantity of 10.0 mg was placed in a 70 µl alumina crucible heated under nitrogen flow (60 ml· min^{-1}). TGA/DSC1 allowed also measuring the mass losses and heats connected to the various chemical and physical transformation of the materials.

2.3.3. Rheological analysis

The processability of the samples was firstly evaluated measuring the Melt Volume Index (MVI) parameter using the M-Flow plastometer (Zwick Roell) and following the standard procedure ISO 1133–1.

Furthermore, the material rheological behavior was assessed using an ARES (TA Instrument) strain-controlled rheometer equipped with a parallel plate geometry (plate diameter = 25 mm, typical gap imposed during the tests = 1 mm).

The complex viscosity curves of the investigated materials were acquired through frequency sweep measurements performed at 200, 230, 260 and 270°C, in the range 0.1–100 rad·s^{-1}. The value of strain amplitude was fixed low enough to ensure the recorded response was within the linear viscoelastic region (determined for each sample through preliminary strain sweep tests) of the materials. Data collected through frequency sweep tests were fitted using the Cross model:

$$\eta^* = \frac{\eta_0^*}{[1 + \lambda\omega]^{1-n}} \quad (1)$$

where: η_0^* is the zero-shear viscosity, λ is the relaxation time, n is the flow index.

Specimens for the rheological characterization were obtained through a two-step procedure. Firstly, the materials were homogenized through compounding in a co-rotating twin screw micro extruder DSM Xplore 15 ml microcompounder (Geleen). The screw speed was maintained at 50 min^{-1} for the feeding stage and increased to 100 min^{-1} for the residence time fixed for all runs at 2 min. The temperature was selected at 190 °C and the processing was carried out under N_2 atmosphere. Then, disk-shape samples (diameter = 25 mm and thickness = 1 mm) were obtained using a hot compression molding press (Collin P 200 T press) working at 190 °C with an applied pressure of 100 bar for 2 min.

2.4. Filament formation and characterization

The extruder used in this study for the production of the filaments was a Next 1.0 Advanced Silver Model (3devo) with the technical characteristics reported elsewhere [25]. According to the supplier indications, this extruder was modified to guarantee a more homogeneous cooling of the PP filament coming out from the die [30]. The cylindrical cooling device was 3D printed in polylactic acid (PLA) and assembled with one of the two fans, in order to avoid the ovalization of the PP filament due to its anisotropic crystallization during cooling [26].

For each sample, preliminary tests were carried out in order to optimize the process conditions. The initial parameters were set considering both those reported in literature about FFF process with PP [30,31] and the results obtained from the chemical and physical characterization of the samples. Then, the optimum parameters of the extrusion process, such as temperature, fan speed and screw speed, were found through a step-by-step approach.

The measurement of the filament diameter was assessed in real-time during the extrusion using the 3devo software, DevoVision, Furthermore, in order to provide the general appearance and to highlight defects, such as the presence of foreign materials, bubbles and roughness, the filaments underwent stereomicroscopic analysis with a SMZ-171 (Motic) instrument. In particular, the filaments were examined at magnifications of 10x, 30x and 40x.

Morphology of the filaments was analyzed using a Zeiss (Oberkochen) VP Scanning Electron Microscope (beam voltage: 20 kV). Prior to observation, the filaments were cryogenically fractured in liquid nitrogen and the obtained surfaces were gold metallized with Gold Sputter Coater-Emitech K550.

Lastly, an Alliance RT/50 (MTS Systems) was used for the static mechanical tensile tests directly on the filaments (length of the sample = 150 mm), using a 2 kN load cell with the crosshead speed at 1 mm·min^{-1} (displacement control test). The mechanical tensile tests were carried out also on some PP-based commercial 3D filaments for comparison. Five samples were tested for each type of filament and the results were reported as average values.

2.5. 3D printing and quality control of the printed parts

The 3D printer used in this study is the Creality Ender-3 Pro, with a Plexiglas box built around the printer to guarantee a uniformly warm printing chamber [30]. Since most of PP-based filaments are characterized by a high crystallinity grade which favours the warpage and/or adhesion of the material on the bed machine (i.e. the printing platform),

the 3D printer bed was covered with a PP-based scotch tape to improve the adhesion of the fused PP filament, as suggested by many authors [26, 32]. This solution contributes to avoid a possible delamination of the first layer deposited by the 3D printer bed.

A little hexagonal bolt with blunt edges and with side and inner circumference diameter of 13 mm and height of 9.1 mm, respectively, was designed with the Autodesk® Fusion 360 modeling software. The label "PP" was introduced to evaluate the definition of a small engraving and to give the opportunity to separately collect and recycle the printed objects at a later time (Figure S1). The software used to obtain g-code was Ultimaker Cura version 4.7.0.

The fan speed (Fan_s = 50%), the printing speed (P_s= 60 mm·s^{-1}), the infill (Infill= 20%), the flow rate (F_{rate}=106%) and the layer thickness (0.2 mm) were kept constant during all the tests. For each material the initial 3D printing parameters were derived from the optimal conditions found during the extrusion and the thermal/rheological results. During the tests, some parameters were adjusted to achieve the best 3D printing conditions. The same specimen was also printed with PP-based commercial filaments (PLene T15 TREED Filament and Centaur PP Form-Futura), for a qualitative comparison, setting the parameters as suggested by manufacturers.

From simple lines to more complex geometric shapes, infill patterns can affect the characteristics of the specimens, such as morphology, mechanical properties, weight and even flexibility as well as the printing time. Thus, concentric, and cubic pattern were considered for the trials. Concentric pattern is quick to print, good for flexible parts, and consumes significantly less material than most patterns, while the cubic one, provides excellent mechanical strength in three dimensions but takes more material and time.

The 3D printed bolts underwent the morphological analysis with an optical microscope instrument in order to highlight defects, resolution and definition. The sample was examined with magnifications of 50–100X.

3. Results and discussion

3.1. Characterization of WEEE samples

Fig. 2 reports the FTIR spectrum of the WEEE material. The collected spectrum confirmed that the sample was made of PP; in fact, it can be observed the presence of the characteristic peaks in the two broad ranges from 2838 to 2952 cm^{-1} (associated with the symmetric and asymmetric stretching of CH_2 and CH_3) and from 1372 to 1456 cm^{-1} (attributed to the bending of CH_3) [30]. The large band at 1014 cm^{-1}, ascribable to siloxane bond functional group (Si-O), revealed that the WEEE sample was also characterized by the presence of a significant amount of talc [33]. In fact, talc is often used as an inorganic filler for PP to improve its processability [20,26] and its mechanical properties [34]. Since the absorbance of the siloxane band was variable among the different scraps, the sample was divided in two different streams, namely PP-WEEE-HA and PP-WEEE-LA, on the basis of different contents of talc according to the value of absorbance greater or less of 0.3, respectively) of the functional group Si-O. From now, the subsequent characterization of the two WEEE samples was carried out separately. In conclusion, the WEEE sample was divided into three portions: PP-WEEE-HA (67 wt%), PP-WEEE-LA (25 wt%) and other plastic waste (8 wt%). The latter was composed of heavily dirty PP scraps and foreign materials, such as other plastics and metals and it was rejected.

3.2. Ultimate and proximate analysis

Table 2 reports the elemental composition and the ash content of the PP-WEEE samples. The proximate analysis showed that the two samples were characterized by different quantities of talc (measured as ash content: 27.5 wt% and 13.3 wt% for PP-WEEE-HA and PP-WEEE-LA, respectively), thus confirming the separation carried out through the FTIR analysis. Instead, the low water content confirmed the hydrophobicity of this plastic material. The high ash content conditioned the values of ultimate analysis, which are significantly lower in comparison to those of a commercial PP as reported in a previous work [25], but the C/H ratio of the WEEE samples were very similar to that of a pristine PP sample (5.9 versus 5.8, respectively).

3.3. Thermal behaviour

TG/DSC simultaneous tests were performed prior to the study of the processability of the materials, in order to evaluate the thermal behaviour of the samples, as well as their processing window. The resulting TG, DTG and DSC profiles of the two PP-WEEE samples were plotted in Fig. 3, while Table 3 reports the values of their main thermal characteristics.

Both WEEE samples showed an endothermic peak centered at 166 °C, associable with the melting of the α−form crystals of PP (Fig. 3a) [35]. The second endothermic peak is associated to a mass variation and corresponds to the thermal degradation of the polymer. The performed tests can give useful information about the extrusion process of the materials, since it is important to keep away from temperatures corresponding to the beginning of degradation step ($T_{d,i}$) (or to the beginning of the first one, if more degradation peaks are present) in order to avoid producing an exhausted, or worst, a partially degraded filament. Considering the initial degradation temperatures, some important differences were observed between the two samples. More specifically, $T_{d,i}$ of PP-WEEE-HA and PP-WEEE-LA was 380 °C and 401 °C, respectively (Fig. 3b-c). Furthermore, the mass losses over this temperature range

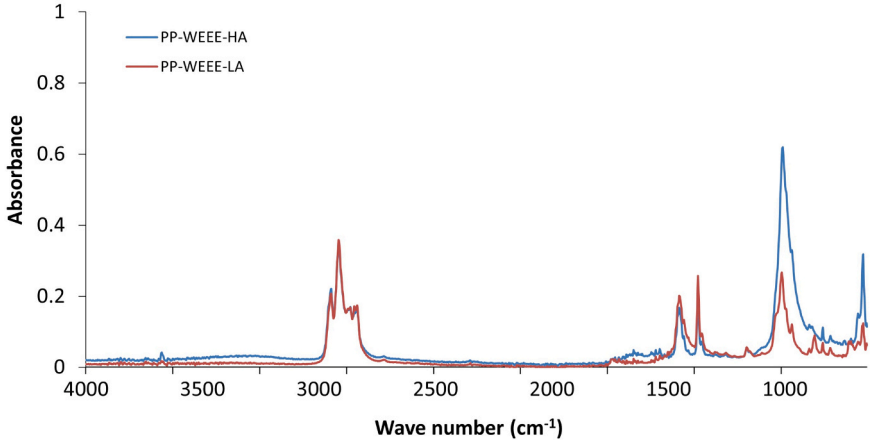

Fig. 2. FTIR spectra of the two samples PP-WEEE-HA and PP-WEEE-LA.

Table 2
Ultimate analysis, water content and ash content of PP-WEEE samples.

Sample	Proximate analysis (wt%)		Ultimate analysis (wt%)*					Halogens analysis (wt%)	
	Water content	Ash	C	N	H	S	O**	Br	Cl
PP-WEEE-HA	0.28 ± 0.01	27.49 ± 0.05	59.0 ± 0.2	n.d.	10.11 ± 0.02	n.d.	3.38	n.d	n.d
PP-WEEE-LA	0.14 ± 0.05	13.3 ± 0.5	71.0 ± 0.2	n. d.	11.9 ± 0.1	n.d.	3.81	0.03 ± 0.006	n.d

Notes:
n.d.: not detected
* on dry basis
** by difference

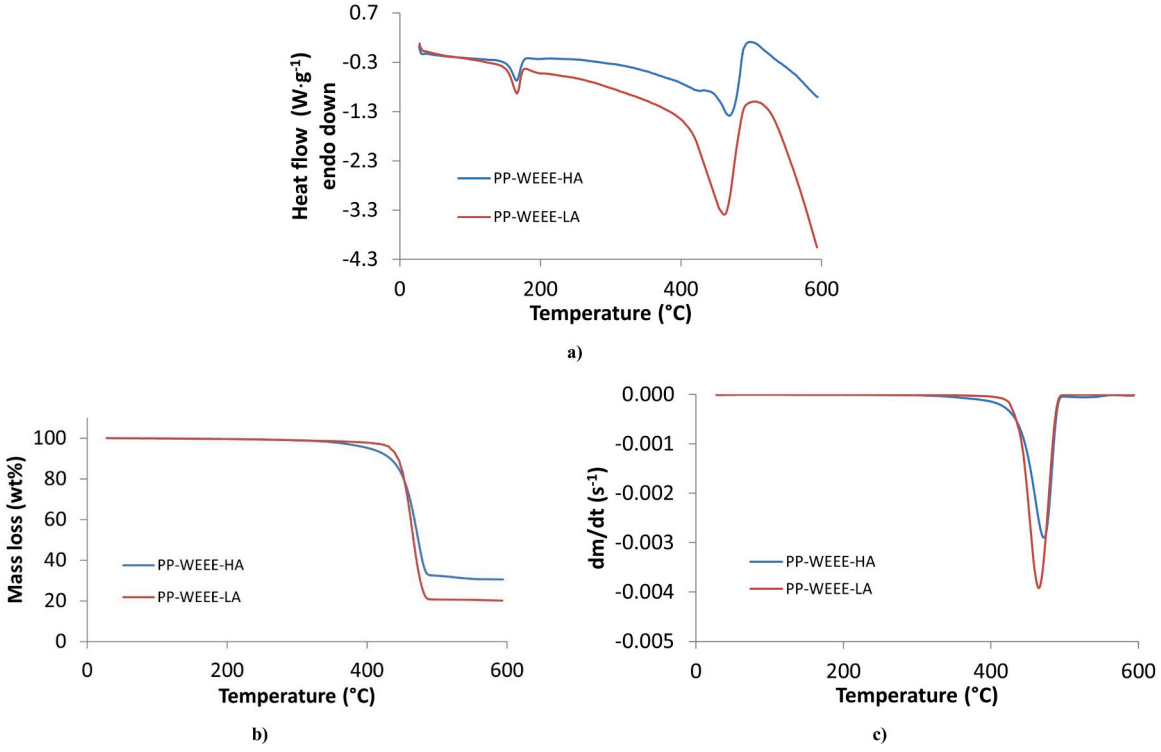

Fig. 3. DSC (a), TG (b) and DTG (c) curves of PP-WEEE-HA and PP-WEEE-LA in the temperature range 25–600 °C, under N_2.

Table 3
Thermal properties of WEEE samples.

Sample	$T_{m,1}$ (°C)	$Q_{m,1}$ (J·g^{-1})	$T_{d,i}$ (°C)	$T_{d,p}$ (°C)	Q_d (J·g^{-1})	Δm 25 °C ÷ $T_{d,i}$ (wt%)
PP-WEEE-HA	166 ± 0.2	56 ± 0.3	380 ± 1	469 ± 3	168 ± 51	5.0 ± 0.5
PP-WEEE-LA	167 ± 0.6	52 ± 1	401± 0.1	467 ± 2	605 ± 52	2.3 ± 0.1

Notes:
T_m: melting temperature;
Q_m: heat of fusion;
Q_d: heat of degradation;
$T_{d,i}$: initial degradation temperature;
$T_{d,p}$: degradation peak temperature.

were 5 and 2.3 wt%, respectively, and the Q_d of PP-WEEE-HA much lower than that of PP-WEEE-LA (Table 3). Therefore, PP-WEEE-LA appeared to be more stable at high temperatures than PP-WEEE-HA although the $T_{d,p}$ of all samples are very similar. In any case, both systems can be considered stable at the typical working conditions of the process of filament formation (carried out at about 180–200°C) and of the 3D printing (performed at 250–265°C). Table S2 shows the results of thermal analysis carried out on the commercial filaments for comparison and the relative discussion.

3.4. Rheological characterization of WEEE samples

Aiming at evaluating the processability of the PP-WEEE samples through FFF, the MFI of the two samples has been evaluated. The obtained results, listed in Table 4, highlight a remarkable difference between the evaluated materials. PP-WEEE-HA sample shows a significantly lower value of MFI than PP-WEEE-LA, likely according to the high content of talc in this sample, as already demonstrated by FTIR and TGA characterizations. From the comparison of the obtained values with those reported on the technical datasheets of some commercial filaments for FFF, such PP-Centaur, PLene or NEVIPROP 040 TL40, it is clear that these filaments present a MFI of 8, 12 and 12.5 respectively.

Table 4
MFI values for PP-WEEE-LA and PP-WEEE-HA samples.

Sample	MFI
PP-WEEE-HA	5.47 ± 0.03
PP-WEEE-LA	13.10 ± 0.40

Based on these values, it can be inferred that PP-WEEE-LA should exhibit a good level of extrudability during the FFF process. However, for a successful 3D printing of PP-WEEE-HA, a more accurate optimization of the process conditions could be required.

In order to deeply investigate the rheological behavior of the two materials, dynamic rheological analyses were carried out. Fig. 4(a-b) report the complex viscosity curves as a function of frequency for PP-WEEE-LA and PP-WEEE-HA, respectively, evaluated at different temperatures. As far as the rheological behavior of PP-WEEE-LA sample is concerned (Fig. 4a), it can be observed that at low temperatures the material shows a Newtonian behavior, involving an almost constant viscosity in the low frequency region. This behavior is typically observed in unfilled polymers or in polymer-based composites containing low loadings of micrometric-sized fillers [36]. Interestingly, a progressive increase of the testing temperature causes the appearance of a yield stress behavior in the low frequency region. As widely reported in the literature, this behavior can be associated with the re-arrangement of the filler embedded in the polymer matrix. This effect is usually covered by the rheological response of the high viscosity matrix and tends to become more easily observable when the rheological test is carried out at temperatures high enough to reduce the viscosity of the polymer [37,38].

It is interesting to highlight that the appearance of the yield stress behavior at high temperature is beneficial for the successive processing of the material through FFF. In fact, as reported in the literature [39,40], such kind of behavior is imperative for achieving a good dimensional stability of the filament exiting the printing nozzle, in the so-called stand-off region, and also during the post-deposition step. In particular, the rapid increase of the viscosity of the material in quasi-zero shear conditions ensure the maintenance of the shape of the extruded filament for the whole stand-off region and under the stress generated by the layer-by-layer deposition in the deposition stage [26,41]. Since progressively increasing values of yield stress are obtained with increasing the temperature, a high printing temperature should favor the achievement of more regular and undeformed printed parts.

Looking at the complex viscosity curves of PP-WEEE-HA reported in Fig. 4b, a different behavior can be observed. In fact, likely due to the high average molecular weight of the polymer matrix and to the higher loading of talc as compared to PP-WEEE-LA, this material shows a marked non-Newtonian behavior in the whole investigated frequency range. Also in this case, an increase of the testing temperature induces the appearance of a yield stress behavior at the lowest inspected frequencies, although this phenomenon is less pronounced as compared to PP-WEEE-LA sample.

3.5. Mechanical recycling of PP-WEEE

3.5.1. Filament formation process and filament optimization

Firstly, the optimization of the process parameters was carried out for PP-WEEE-HA sample, varying the heaters temperatures, the cooling fan speed and screw speed. Despite the presence of high talc content, the pronounced volumetric shrinkage of PP, which results in the rapid deformation of the filament during its formation, could still be evident. Consequently, the initial configuration of the extruder was set based on the results derived from other PP materials (encompassing both virgin and waste samples) using the same extruder [26,30].

Table 5 summarizes the evaluated setting parameters of each test, as well as an assessment of the quality of the produced filaments.

In the first test (i.e. I_{HA}), it was observed that the molten sample flowed very slowly, and it was quite solid at the nozzle. Thus, in the II_{HA} test, a progressive increasing temperature of H4 and H3 and a higher screw speed were set. The quality of the filament resulted improved in comparison to the previous one, notwithstanding some ovalization phenomena and the presence of some not melted inclusions (probably due to a non-uniform fusion of loaded particles of slightly different sizes) occurred.

To overcome these issues, in the III_{HA} test, an additional increase of temperatures was set for H4 and H3, that was balanced by a small increase of the fan speed inducing a faster solidification of the material. Since a fast cooling could worsen the quality of the filament, which tend to become oval if the fan speed is too high, the screw speed was lowered to the value of 2.5 min^{-1}. The resulting filament showed a smooth surface and a very stable diameter. The average diameter measured during the whole spooling process was 1.74±0.07 mm, and the value of this standard deviation was fully comparable with the tolerance allowed for the commercial filaments.

The best parameters found for PP-WEEE-HA were also used for PP-WEEE-LA (Table 6). Unfortunately, with these test conditions (I_{LA}), the material extruded was still quite solid and the produced filament showed a high rigidity, although the rheological analyses had highlighted a lower viscosity value for this sample than that of PP-WEEE-HA. However, it is worth noting that the rheological behavior of the two materials was evaluated at a shear rate lower than what is typically experienced during the filament extrusion step. In fact, considering the used processing conditions, the actual shear rate is in the order of 10^3-10^4 s^{-1} [26]. Since these values exceed the shear rate achievable by a rotational rheometer, the complex viscosity curves reported in Fig. 4 (a-b) were fitted through the Cross model (Eq. (1)) to provide information about the viscosity value of the two samples at the actual shear rate experienced during the processing. The obtained results (reported

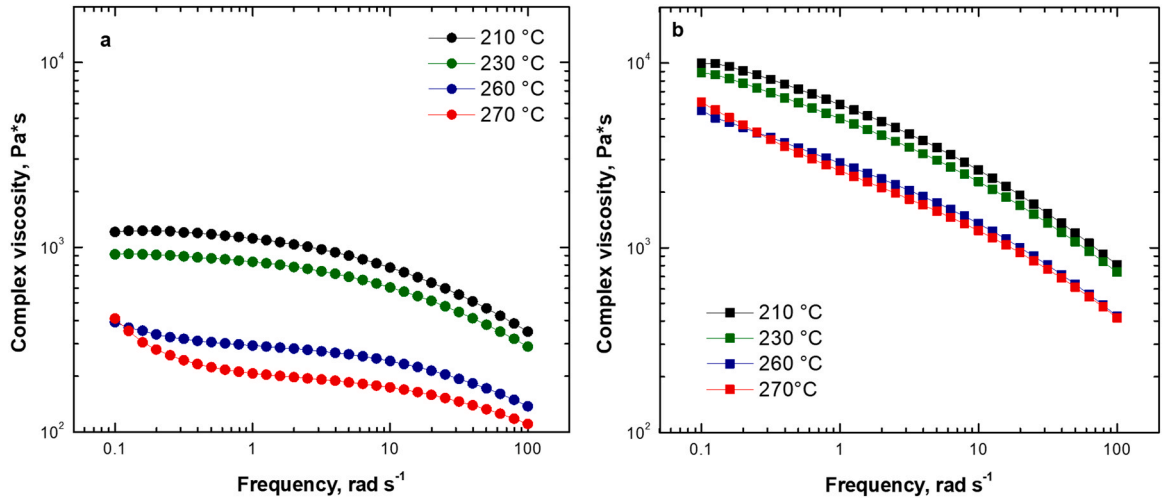

Fig. 4. Complex viscosity curves as a function of frequency evaluated at different temperatures for (a) PP-WEEE-LA and (b) PP-WEEE-HA.

Table 5
Setting parameters of extrusion and visual appearance of the filaments produced from PP-WEEE-HA (H1 ÷ H4 indicate the heating zones from the nozzle to the hopper).

Test/ Filament	H4 (°C)	H3 (°C)	H2 (°C)	H1 (°C)	Fan speed (%)	Screw speed (min^{-1})	Visual appearance/Quality	Printability
I_{HA}	180	180	180	180	15	2.7	Flattend filament with irregular diameter / Scarce	No
II_{HA}	184	182	180	178	15	5	Partially ovalized filament with small unmelted inclusions / Good	Yes
III_{HA}	186	184	180	178	18	2.5	Circular diameter with smooth surface / Excellent	Yes

Table 6
Setting parameters of extrusion and visual appearance of the filaments from PP-WEEE-LA.

Test/Filament	H4 (°C)	H3 (°C)	H2 (°C)	H1 (°C)	Fan speed (%)	Visual appearance/Quality	Printability
I_{LA}	186	184	180	178	18	Rigid filament/ Scarce	No
II_{LA}	190	186	184	182	10	Ovalized filament with a very rough surface/ Scarce	No
III_{LA}	205	200	195	190	5	Circular diameter, rough surface / Good	Yes

[a]the screw speed was maintained constant at 2.5 min^{-1}.

in Fig. S2), showed that at the shear rate that the polymer undergoes during the filament formation process, the sample containing a high amount of talc, presents a lower viscosity than the other one, because of the more pronounced shear thinning behavior of PP-WEEE-HA as compared to PP-WEEE-LA. Therefore, a higher processing temperature is required for PP-WEEE-LA to obtain a regular filament.

Then, test II_{LA} was carried out increasing the temperatures of the heaters and lowering the fan speed to guarantee a uniform melting inside the extruder. The resultant filament presented an improved quality, but it was characterized by a very rough surface and an overall visible instability of the geometrical section (ovalized). Thus, in test III_{LA} the heaters temperatures were further increased and the fan speed was halved. The produced filament had a stable diameter (average value: 1.75±0.08 mm) but the surface was still quite rough, likely due to the lower amount of talc of the sample [27]. Fig. S3 shows the spool with the produced filaments.

To evaluate the circularity and the diameter of the obtained filaments, SEM analysis were performed and some representative micrographs are reported in Fig. 5. The micrographs of filaments III_{HA} documented the achievement of a smooth and homogenehous surface, a quite circular section as well as a minimum variation of the diameter along the filament (Fig. 5a). Otherwise, III_{LA} (Fig. 5b) was characterized by a rough surface and a not perfectly circular section. These results are already evident through the observation with the stereomicroscope (Fig. S4). It is important to highlight that, despite the typical intrinsic heterogeneity of the se recycled materials, the filaments did not present porosity or evident inclusions of foreign materials or impurities. Therefore, both filaments are suitable for the subsequent 3D printing process, notwithstanding some irregularities in the external surface of the III_{LA} sample, which can be attributed to the more difficult processability of this material as compared to III_{HA}.

The mechanical properties of the filaments produced with the

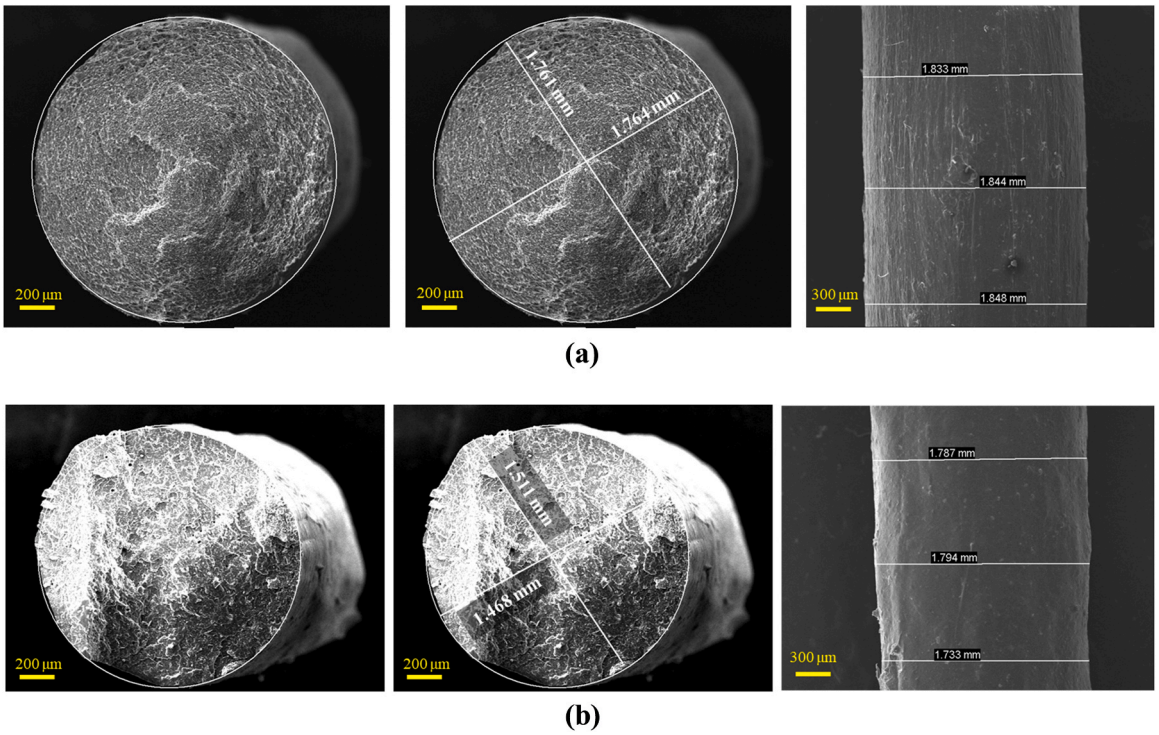

Fig. 5. SEM micrographs of cross section and side surface of (a) III_{HA} and (b) III_{LA} filaments.

process conditions III_{HA} and III_{LA} were assessed through tensile tests, and the results were compared with those obtained from two commercial filaments, PP-Centaur and PLene. The values of tensile strength, elastic modulus and breaking deformation are shown in Table 7. Furthermore, in Fig. S6 an example of stress-strain curve for each sample and commercial filament was provided.

Overall, the mechanical properties of III_{HA} and III_{LA} were comparable to those of the commercial filament PLene. The elastic modulus and tensile strength of PP-WEEE samples are affected by the presence of the embedded fillers and higher values were obtained for the material with high content of talc (test III_{HA}), in accordance with the literature concerning the mechanical properties of polymer composites filled with talc [42]. Since PLene and PP-WEEE-LA have a similar amount of talc (Table S1 and Fig. S5), the above-mentioned parameters were comparable. Concerning the values of the elongation at break, PP-WEEE samples exhibited lower values as compared to commercial filaments. To explain this result, it should be considered that PP-WEEE samples are intrinsically heterogeneous mixture of different PPs (as usual for plastics collected in WEEE-MRFs). Furthermore, the mechanical properties of the PP-WEEE materials could be affected by the degradation or aging processes underwent by the polymers during their life span.

3.5.2. 3D printing test and optimization

Similarly, to the filament making process, different tests have been carried out for the optimization of the 3D printing process by varying the diameter of the nozzle and the infill patterns (i.e. cubic or concentric). Furthermore, in-depth observations about the shape and layer-by-layer deposition were done through the optical microscope instrument to evaluate the 3D printing quality.

The printing setup and a qualitative evaluation of the specimens in PP-WEEE-HA are shown in Table 8. Bed and nozzle temperatures were kept constant (T_{bed}=110°C; T_{nozzle}=250°C).

The temperature of the nozzle was chosen in accordance with the rheological behavior of PP-WEEE-HA, but also considering previous studies regarding the FFF process of PP-based talc filled materials [26]. Even if the material regularly flows through the nozzle and appeared suitable for 3D printing in each tested condition, the reduction of the nozzle diameter led to reach a better quality of the printed parts.

In fact, in the first test, an over-extrusion was visible on the top-layer at the end of the process, as observable in the picture reported in Fig. 6a and in the micrographs obtained at the optical microscope depicted in Fig. S7a. The gradual reduction of the nozzle diameter from 0.6 to 0.5 and 0.4 mm (tests III_{HA}-2,3,4) induced a progressive improvement in the quality of printed parts (see Figs. 6b, c, d and S7b, c, d). It is possible to observe that the deposition of the layers and the details of the label were gradually improved in the bolts printed using nozzle with progressively low diameter. In fact, the best quality was reached for the specimens printed using the III_{HA}-3 and III_{HA}-4 conditions, where the use of both concentric and cubic infill pattern was tested. Even if the label was not affected by this parameter, a better deposition was observed with the cubic infill (Fig. S7d), likely due to the deposition of more material and a longer printing time.

Starting from the conditions set for the best performed bolts (test III_{HA}-3), tests with filament III_{LA} were carried out (Table 9). On the basis of the considerations about the rheological behavior of PP-WEEE-LA reported in paragraph 3.5.1, the T_{nozzle} was increased of 10 °C (T_{nozzle} = 260°C) while T_{bed} was kept constant at 110°C. From the first test (i.e. III_{LA}-1, Fig. 6e), the printed bolt showed a good quality but with a slight phenomenon of stringing (Fig. S7e). Besides, the deposition of the layers and the label were characterized by some visible minor imperfections. This is probably due to the surface roughness of the filament. However, this surface roughness never caused difficulties during the printing process. Thus, a second test was performed to improve the quality of the bolt, reducing the stringing effect [30]. The III_{LA} −2 test was performed with a slight increase of the T_{nozzle} at 265°C, which guaranteed that the filament was able to follow the printing pattern. As can be observed in Fig. 6f, the stringing effect was no longer present in the relative bolt. Finally, the combination of this parameter and the appropriate retraction distance enable the achievement of optimal resolution both for the layers overlap and the label (Fig. S7f).

Lastly, the bolt III_{HA}-3 and III_{LA}-2 were compared with the same specimen printed with the PP-Centaur (Fig. 6g) and PLene filaments (Fig. 6h). The two relative bolts were comparable in terms of visible quality to those realized with recycled PP. Finally. it was qualitatively evaluated that some slight visible defects (e.g. low details definition, imperfection of layers adhesion, stringing, etc.) were very similar in all the printed bolts. Despite the use of recycled materials, the surface of the specimens was comparable to that of the same specimens printed with PLene or with Centaur.

Table 7
Mechanical properties of the filaments III_{HA} and III_{LA} (from WEEE) and PLene and PP-Centaur (commercial filaments).

Filament	Tensile strength (MPa)	Elastic modulus (MPa)	Elongation at break (%)
III_{HA}	19.7±0.5	1837±137	52.3±13.9
III_{LA}	21.4±1.8	1379±337	10.7±4.2
PLene	18.9±0.7	1309±177	> 100
PP-Centaur	10.8±0.2	341±19	> 100

Table 8
3D printing parameters and visual appearance of the printed specimen for PP-WEEE-HA.

Test	Nozzle diameter (mm)	Infill pattern	Final visible quality
III_{HA} −1	0.6	Cubic	Poor
III_{HA} −2	0.5	Concentric	Good
III_{HA} −3	0.4	Concentric	Optimal
III_{HA} −4	0.4	Cubic	Optimal

Constant parameters: T_{bed}=110°C; T_{nozzle}=250°C; Infill=20%; Ps=60 mm·s^{-1}; Fans=50%; F_{rate}=106%; layer thickness=0.2 mm.

4. Conclusion

This study presents a promising approach to the recycling of plastic waste from WEEE by means the production of filaments suitable for 3D printing processes. The plastic scraps, predominantly composed of PP filled with talc particles, were obtained from various devices, resulting in a range of talc content. Therefore, the stream was divided in two samples namely, PP-WEEE-LA and PP-WEEE-HA containing 13.3 and 27.5 wt% of talc, respectively. The assessment of the rheological behavior of both samples demonstrated the beneficial effect of the talc in inducing non-Newtonian features, such as yield stress and shear thinning, which are key requirements for the successful FFF processability of thermoplastic materials.

Filaments based on both WEEE streams were obtained after optimizing the process conditions.

The results indicated that the filaments achieved a homogeneous surface (especially for the filament based on PP-WEEE-HA), a quite circular section, and were characterized by mechanical properties comparable to those of PP-based commercial filaments. Finally, the 3D printed specimens, obtained through an optimized FFF, showed satisfactory resolution and definition when compared qualitatively with those obtained using commercial filaments.

The successful production of 3D printing filaments from WEEE suggests the potential development of a circular economy strategy in the EEE industry. In future perspectives, this research delineates a new approach for the recycling of PP-WEEE, making it suitable candidate for filament production for 3D printing. Given the noteworthy properties of this polymer, future investigations could focus on optimizing the filament production process for prototyping. Furthermore, this might be

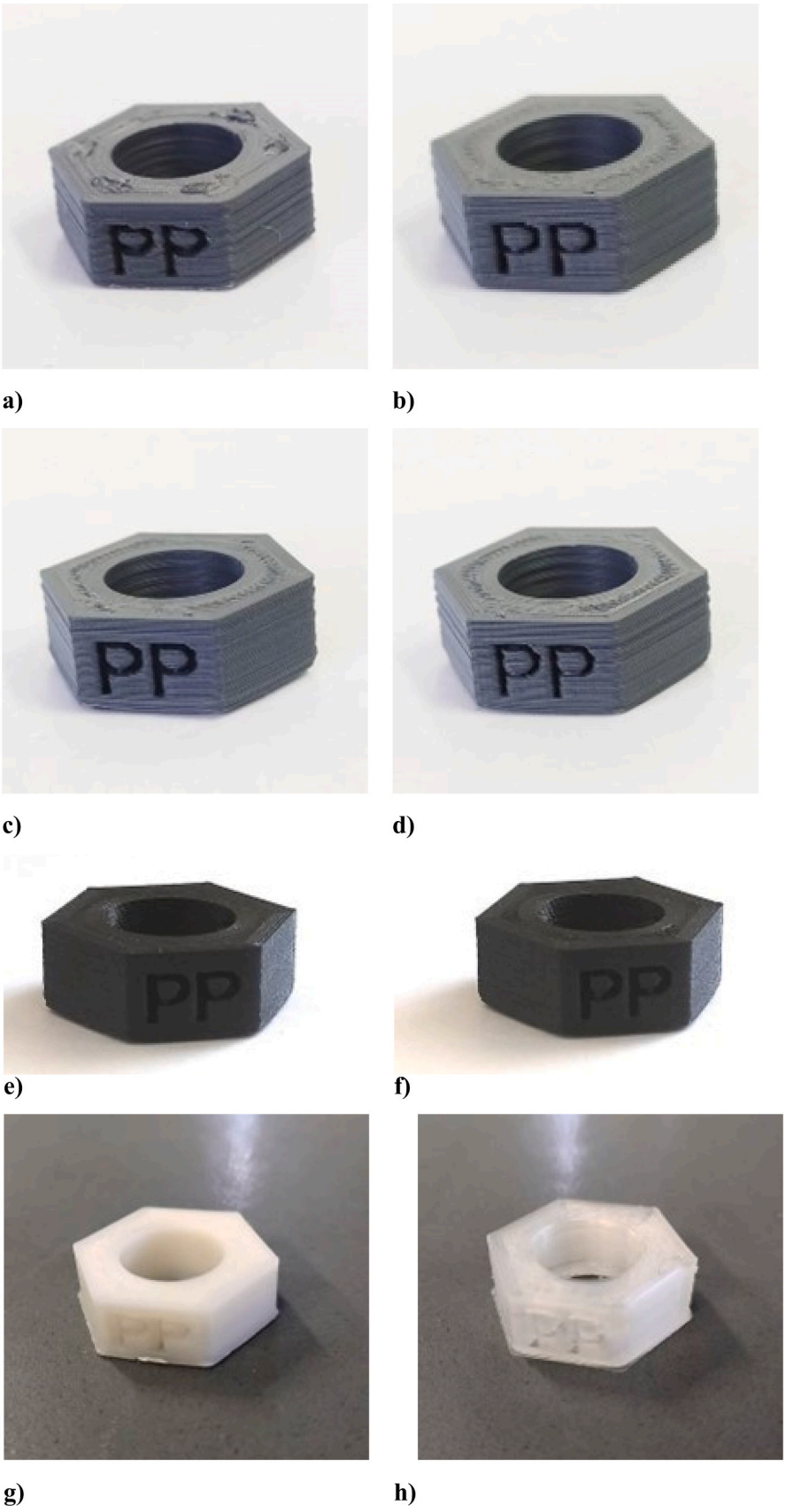

Fig. 6. Printed bolt: Test III_{HA}-1 (a); Test III_{HA}-2 (b); Test III_{HA}-3 (c); Test III_{HA}-4 (d); Test III_{LA}-1 (e); Test III_{LA}-2 (f). Test PP-Centaur (g); Test PLene (h).

Table 9
3D printing parameters and visual appearance of the printed specimen for PP-WEEE-LA.

Test	T_{nozzle} (°C)	Final visible quality
III_{LA} −1	260	Good (presence of some stringing)
III_{LA} −2	265	Optimal

Constant parameters: Ps=60 mm·s^{-1}; Fans=50%; layer thickness=0.2 mm, Infill=20%; F_{rate}=106%; T_{bed}=110°C; nozzle diameter=0.4 mm

accomplished in conjunction with assessing the mechanical properties of larger 3D printed objects. Such efforts could culminate in the production of high-quality recycled plastic items, thereby mitigating the environmental impact of electronic waste, and contributing to sustainable manufacturing practices.

Funding

This work was supported by the Agenzia nazionale per le nuove tecnologie, l'energia e lo sviluppo economico sostenibile (ENEA) through "5×1000" 2019 funds: Progetto Zero Plastica.

CRediT authorship contribution statement

Letizia Tuccinardi: Writing – original draft, Methodology, Investigation, Conceptualization. **Alberto Frache:** Writing – review & editing, Supervision. **Riccardo Tuffi:** Writing – review & editing, Project administration, Conceptualization. **Rossella Arrigo:** Writing – review & editing, Writing – original draft, Methodology, Investigation. **Andrea Spirio:** Investigation.

Declaration of Competing Interest

The authors declare that they have no known competing financial interests or personal relationships that could have appeared to influence the work reported in this paper

Data availability

Data will be made available on request.

Acknowledgment

The authors wish to thank Puli Ecol Recuperi S.r.l. (MC) for the supply of WEEE plastics, Dr Roberto Terzi and Mr. Filiberto Valentino of ENEA for their technical support for the mechanical analysis.

Appendix A. Supporting information

Supplementary data associated with this article can be found in the online version at doi:10.1016/j.jece.2024.112474.

References

[1] C. Jirang, E. Forssberg, Mechanical recycling of waste electric and electronic equipment: a review, J. Hazard. Mater. Volume 99 (Issue 3) (2003) 243–263, https://doi.org/10.1016/S0304-3894(03)00061-X.
[2] A. Merlo, L. Lavagna, D. Suarez-Riera, M. Pavese, Recycling of WEEE plastics waste in mortar: the effects on mechanical properties, Recycling 6 (2021) 70, https://doi.org/10.3390/recycling6040070.
[3] X. Meng, Y. Li, N. AlMasoud, W. Wang, T.S. Alomar, J. Li, X. Ye, H. Algadi, I. Seok, H. Li, B.Bin Xu, N. Lu, Z.M. El-Bahy, Z. Guo, Compatibilizing and toughening blends of recycled acrylonitrile-butadiene-styrene/recycled high impact polystyrene blends via styrene-butadiene-glycidyl methacrylate terpolymer, Polymer Volume 272 (2023) 125856, https://doi.org/10.1016/j.polymer.2023.125856.
[4] C.P. Balde, G. Iattoni, C. Xu, T. Yamamoto, Update of WEEE Collection Rates, Targets, Flows, and Hoarding – 2021 in the EU-27, United Kingdom, Norway, Switzerland, and Iceland, 2022, SCYCLE Programme, United Nations Institute for Training and Research (UNITAR), Bonn, Germany.https://weee-forum.org/wp-content/uploads/2022/12/Update-of-WEEE-Collection_web_final_nov_29.pdf.
[5] V. Forti, C. Balde P. Kuehr, R & Bel, G. (2020). The global e-waste monitor 2020: quantities, flows and the circular economy potential. United Nations University (UNU)/United Nations Institute for Training and Research (UNITAR) – co-hosted SCYCLE Programme, International Telecommunication Union (ITU) & International Solid Waste Association (ISWA), Bonn/Geneva/Rotterdam. https://www.itu.int/en/ITU-D/Environment/Documents/Toolbox/GEM_2020_def.pdf.
[6] J.A.P. Silva, G.G. Lima, C.F. Camilo-Cotrim, et al., Impact of E-Waste Toxicity on Health and Nature: Trends, Biases, and Future Directions, Water Air Soil Pollut. 234 (2023) 320, https://doi.org/10.1007/s11270-023-06328-2.
[7] M. Shahabuddin, M.N. Uddin, J.I. Chowdhury, et al., A review of the recent development, challenges, and opportunities of electronic waste (e-waste), Int. J. Environ. Sci. Technol. 20 (2023) 4513–4520, https://doi.org/10.1007/s13762-022-04274-w.
[8] B. Beccagutti, L. Cafiero, M. Pietrantonio, S. Pucciarmati, R. Tuffi, S. Vecchio Ciprioti, Characterization of some real mixed plastics from WEEE: a focus on chlorine and bromine determination by different analytical methods, Sustain. -Basel 8 (2016) 1107–1123, https://doi.org/10.3390/su8111107.
[9] G. Martinho, A. Pires, L. Saraiva, R. Ribeiro, Composition of plastics from waste electrical and electronic equipment (WEEE) by direct sampling, Waste Manag 32 (2012) 1213–1217, https://doi.org/10.1016/j.wasman.2012.02.010.
[10] V. Sahajwalla, V. Gaikwad, The present and future of e-waste plastics recycling, Curr. Opin. Green. Sustain. Chem. 13 (2018) 102–107, https://doi.org/10.1016/j.cogsc.2018.06.006.
[11] S. Tostar, E. Stenvall, M.R.S.J. Foreman, A. Boldizar, The Influence of Compatibilizer Addition and Gamma Irradiation on Mechanical and Rheological Properties of a Recycled WEEE Plastics Blend, Recycling 1 (2016) 101–110, https://doi.org/10.3390/recycling1010101.
[12] J. Maris, S. Bourdon, J.-M. Brossard, L. Cauret, L. Fontaine, V. Montembault, Mechanical recycling: Compatibilization of mixed thermoplastic wastes, Polym. Degrad. Stab. Volume 147 (2018) 245–266, https://doi.org/10.1016/j.polymdegradstab.2017.11.001.
[13] V. Gaikwad, A. Ghose, S. Cholake, A. Rawal, M. Iwato, and, V. Sahajwalla, Transformation of E-Waste Plastics into Sustainable Filaments for 3D Printing, ACS Sustain. Chem. Eng. 6 (11) (2018), https://doi.org/10.1021/acssuschemeng.8b03105.
[14] I. Ilankoon, et al., E-waste in the international context–a review of trade flows, regulations, hazards, waste management strategies and technologies for value recovery, Waste Manag 82 (2018) 258–275, https://doi.org/10.1016/j.wasman.2018.10.018.
[15] C. Chaine, A.S. Hursthouse, B. McLean, I. McLellan, B. McMahon, J. McNulty, J. Miller, E. Viza, Recycling Plastics from WEEE: A Review of the Environmental and Human Health Challenges Associated with Brominated Flame Retardants, Int. J. Environ. Res. Public Health 19 (2022) 766, https://doi.org/10.3390/ijerph19020766.
[16] A. Haarman, F. Magalini, J. Courtois. Study on the Impacts of Brominated Flame Retardants on the Recycling of WEEE plastics in Europe. SOFIES 2020. https://www.bsef.com/wp-content/uploads/2020/11/Study-on-the-impact-of-Brominated-Flame-Retardants-BFRs-on-WEEE-plastics-recycling-by-Sofies-Nov-2020.pdf.
[17] E. Sanchez-Rexach, T.G. Johnston, C. Jehanno, H. Sardon, A. Nelson, Sustainable Materials and Chemical Processes for Additive Manufacturing, Chem. Mater. 32 (17) (2020) 7105–7119, https://doi.org/10.1021/acs.chemmater.0c02008.
[18] D. Wang, T. Zhang, X. Guo, D. Ling, L. Hu, G. Jiang, The potential of 3D printing in facilitating carbon neutrality, J. Environ. Sci. Volume 130 (2023) 85–91, https://doi.org/10.1016/j.jes.2022.10.024.
[19] P.K. Penumakala, J. Santo, A. Thomas, A critical review on the fused deposition modeling of thermoplastic polymer composites, Compos. B Eng. 201 (2020) 108336, https://doi.org/10.1016/j.compositesb.2020.108336.
[20] R. Arrigo, D. Battegazzore, G. Bernagozzi, F. Cravero, D.N. Ribero Pedraza, A. Frache, Recycled PP for 3D Printing: Material and Processing Optimization through Design of Experiment, Appl. Sci. 12 (2022) 10840, https://doi.org/10.3390/app122110840.
[21] S. Chong, G.-T. Pan, M. Khalid, T. C.-K.Yang, S.-T. Hung, C.-M. Huang, Physical Characterization and Pre-Assessment of Recycled High-Density Polyethylene as 3D Printing Material, J. Polym. Environ. 25 (2) (2017) 136–145, https://doi.org/10.1007/s10924-016-0793-4.
[22] N.E. Zander, Recycled Polymer Feedstocks for Material Extrusion Additive Manufacturing. In Polymer-Based Additive Manufacturing: Recent Developments, ACS Symp. Ser. 1315 (2019) 37–51, https://doi.org/10.1021/bk-2019-1315.ch003.
[23] J.D. Kechagias, D. Chaidas, Fused filament fabrication parameter adjustments for sustainable 3D printing, Mater. Manuf. Process. (2023), https://doi.org/10.1080/10426914.2023.2176872.
[24] M.I. Mohammed, D. Wilson, E. Gomez-Kervin, A. Petsiuk, R. Dick, J.M. Pearce, Sustainability and feasibility assessment of distributed E-waste recycling using additive manufacturing in a Bi-continental context (Article), Addit. Manuf. 50 (2022) 102548, https://doi.org/10.1016/j.addma.2021.102548.
[25] L. Cafiero, D. De Angelis, M. Di Dio, P. Di Lorenzo, M. Pietrantonio, S. Pucciarmati, R. Terzi, L. Tuccinardi, R. Tuffi, A. Ubertini, Characterization of WEEE plastics and their potential valorisation through the production of 3D printing filaments, J. Environ. Chem. Eng. Volume 9 (Issue 4) (2021) 105532, https://doi.org/10.1016/j.jece.2021.105532.

[26] M. Bertolino, D. Battegazzore, R. Arrigo, A. Frache, Designing 3D printable polypropylene: material and process optimisation through rheology, Addit. Manuf. 40 (2021) 101944, https://doi.org/10.1016/j.addma.2021.101944.
[27] G. Bernagozzi, D. Battegazzore, R. Arrigo, A. Frache, Optimizing the Rheological and Thermal Behavior of Polypropylene-Based Composites for Material Extrusion Additive Manufacturing Processes, Polymers 1 (2023) 2263, https://doi.org/10.3390/polym15102263.
[28] L. Cafiero, D. Fabbri, E. Trinca, et al., Thermal and spectroscopic (TG/DSC–FTIR) characterization of mixed plastics for materials and energy recovery under pyrolytic conditions, J. Therm. Anal. Calor. 121 (2015) 1111–1119, https://doi.org/10.1007/s10973-015-4799-2.
[29] L. Sun, X. Zeng, J. Li, Pollutants release and control during WEEE recycling: A critical review, Procedia Environ. Sci. 31 (2016) 867–872, https://doi.org/10.1016/j.proenv.2016.02.100.
[30] G. Occasi, D. De Angelis, M. Scarsella, Mo Tammaro, L. Tuccinardi, R. Tuffi, Recovery material from a new designed surgical face mask: A complementary approach based on mechanical and thermo-chemical recycling. https://doi.org/10.1016/j.jenvman.2022.116341.
[31] M. Jin, C. Neuber, H.-W. Schmidt, Tailoring polypropylene for extrusion-based additive manufacturing, Addit. Manuf. 33 (2020) 101101, https://doi.org/10.1016/j.addma.2020.101101.
[32] M. Spoerk, C. Holzer, J. Gonzalez-Gutierrez, Material extrusion-based additive manufacturing of polypropylene: A review on how to improve dimensional inaccuracy and warpage, J. Appl. Polym. Sci. (2020), https://doi.org/10.1002/APP.48545.
[33] E. Jubete, C.M. Liauw, K. Jacobson, N.S. Allen, Degradation of carboxylated styrene butadiene rubber-based water born paints. Part 1: Effect of talc filler and titania pigment on UV stability (Pages), Polym. Degrad. Stab. Volume 92 (Issue 8) (2007) 1611–1621, https://doi.org/10.1016/j.polymdegradstab.2007.07.014.
[34] Y. Ryu, J.S. Sohn, B.C. Kweon, S. Woon Cha, Shrinkage Optimization in Talc- and Glass-Fiber-Reinforced Polypropylene Composites, Mater. (Basel) 12 (5) (2019) 764, https://doi.org/10.3390/ma12050764, https://doi.org/10.3390/ma12050764.
[35] B. Luo, S. Xu, J. Yang, Q. Zhang, J. Yu, L. Liu, X. Meng, Temperature Effects on the Crystalline Structure of iPP Containing Different Solvent-Treated TMB-5 Nucleating Agents, Polymers 15 (2023) 514, https://doi.org/10.3390/polym15030514.
[36] R. Chen, W. Zou, H.C. Zhang, G.Z. Zhang, Z.T. Yang, G. Jin, J.P. Qu, Thermal behavior, dynamic mechanical properties and rheological properties of poly (butylene succinate) composites filled with nanometer calcium carbonate, Polym. Test. 42 (2015) 160–167, https://doi.org/10.1016/j.polymertesting.2015.01.015.
[37] G. Gentile, V. Ambrogi, Cerruti P., R. Di Maio, G. Nasti, C. Carfagna, Pros and cons of melt annealing on the properties of MWCNT/polypropylene composites. Polymer. DOI: 10.1016/j.polymdegradstab.2014.08.018.
[38] R. Arrigo, D. Antonioli, M. Lazzari, V. Gianotti, M. Laus, L. Montanaro, G. Malucelli, Relaxation Dynamics in Polyethylene Glycol/Modified Hydrotalcite Nanocomposites, Polymers 10 (2018) 1182, https://doi.org/10.3390/polym10111182.
[39] G.D. Goh, Y.L. Yap, H.J.K.J. Tan, S.L. Sing, G.L. Goh, W.Y. Yeong, Process–Structure–Properties in Polymer Additive Manufacturing via Material Extrusion: A Review, Crit. Rev. Solid State Mater. Sci. 45 (2020) 113–133, https://doi.org/10.1080/10408436.2018.1549977.
[40] A. Sola, Materials Requirements in Fused Filament Fabrication: A Framework for the Design of Next-Generation 3D Printable Thermoplastics and Composites, Macromol. Mater. Eng. 307 (2022) 2200197, https://doi.org/10.1002/mame.202200197.
[41] R. Arrigo, A. Frache, FDM Printability of PLA Based-Materials: The Key Role of the Rheological Behavior, Polymers 14 (2022) 1754, https://doi.org/10.3390/polym14091754.
[42] Hattotuwa G.B. Premalal, H. Ismail, A. Baharin, Comparison of the mechanical properties of rice husk powder filled polypropylene composites with talc filled polypropylene composites, Polym. Test. Volume 21 (Issue 7) (2002) 833–839, https://doi.org/10.1016/S0142-9418(02)00018-1.